Spreading of isolated contrails during the 2001 air traffic shutdown

Patrick Minnis, Louis Nguyen Atmospheric Sciences, NASA Langley Research Center, Hampton, VA USA

> David P. Duda Hampton University, Hampton, VA USA

> > Rabindra Palikonda AS&M, Inc., Hampton, VA USA

Abstract for the 10th Conference on Aviation, Range, and Aerospace Meteorology 13-16 May 2002 Portland, OR

Patrick Minnis, Louis Nguyen
Atmospheric Sciences, NASA Langley Research Center, Hampton, VA 23681

David P. Duda Hampton University, Hampton, VA 23666

> Rabindra Palikonda AS&M, Inc., Hampton, VA 23666

1. INTRODUCTION

Like natural cirrus clouds, contrails can impact climate through their radiative effects. Persistent contrails often form in air with relative humidities with respect to ice (RHI) exceeding 100% but with relative humidities with respect to water (RH) less than 100%. Cirrus cloud formation generally requires RH > 100%. Thus, contrails can form clouds in conditions that would not support the formation of most natural cirrus. Cirrus coverage over the USA grew by 0.010/decade between 1971 and 1996, while declining over other land areas with minimal air traffic 0.017/decade. (Minnis et al. 2001). Determining the contribution of contrails to this increase requires explicit knowledge of the spreading characteristics and formation conditions of persistent contrails. Cirrus coverage resulting from young linear contrails can be estimated with 1-km infrared satellite data (Mannstein et al. 1999), but it is difficult to assess the full impact of contrails because they often spread into non-linear, natural-looking cirrus clouds (Minnis et

Determining the contribution of spreading contrails to cirrus coverage requires geostationary satellite infrared data to track the contrails as they develop. The contribution by individual contrails to the cirrus coverage is difficult to obtain because of the satellite imagery's low resolution. Often, new contrails, especially in high traffic areas over the USA, overlay the spreading contrails exacerbating the discrimination of the spreading contrails. During the September 2001 air traffic shutdown, few aircraft operated over the USA eliminating the primary confusion factor in the contrailcirrus estimation process. Skies over the Midwestern USA were apparently primed for contrail, but not cirrus, formation early during September 12. Only a few military aircraft transited the clear supersaturated air mass resulting in several isolated spreading contrails in a an area normally crossed by 70-80 planes per hour. This paper examines this unique case to better understand the contrail formation and growth conditions and ultimately estimate the amount of cloudiness that would have been generated in normal air traffic.

2. DATA & METHODOLOGY

Four-km data from the Geostationary Operational Environmental Satellite (GOES-8 at 75°W and GOES-10 at 135°W) and 1-km data from the Moderate Resolution Imaging Spectroradiometer (MODIS) on the EOS Terra satellite and the Advanced Very High Resolution Radiometer (AVHRR) on NOAA-14, 15, and 16 are used to characterize the contrails. The areal coverage, microphysical properties, and radiative effects of these contrails are computed for each image available during the lifetimes of these contrails. Vertical profiles of temperature, humidity, and wind speed and direction are used to assess the contrail environment. Soundings taken at 1200 UTC, 12 September 2001 from nearby areas provide detailed descriptions of the conditions while the large-scale perspective is provided by hourly calculations of RHI and contrail formation on a 1° grid from Duda et al. (2002) based on Rapid Update Cycle (RUC; Benjamin et al. 1998).

The contrail optical depth τ and microphysical properties are computed using solar-infrared infrared split-window (SIRS) technique used by Minnis et al. (1998). Longwave radiative forcing is computed as in Palikonda et al. (1998). The SIRS uses the 3.9 or 3.7-µm channel with the 11 (IR) and 12 µm channels to derive τ , effective ice crystal diameter D_e , and cloud temperature, T_c . The value of T_c can also be specified reducing the errors in the microphysical parameters.

3. RESULTS AND DISCUSSION

Figure 1 is an abbreviated sequence of GOES-8 IR images showing the formation and spreading of several contrails over Ohio (OH), Pennsylvania (PA), West Virginia (WV), Virginia (VA), and Maryland (MD) between 0745 UTC and 1545 UTC. The segmented contrail (A, B, C) over southern PA initially formed over OH and western PA between 0800 and 1030 UTC. The two southernmost contrails over WV (E, F) at 1345 UTC were first visible at 1145 UTC, while the one in northern WV (G) became visible in the 1345 UTC image. A shortlived trail evident over northern MD (D) at 1145 UTC fades by 1315 UTC. A few additional contrails formed over northern VA and MD are evident at 1445 UTC. The imagery in Figs. 2 and 3 show several of these contrails at high resolution early and late, respectively, in the

^{*}Corresponding author address: Patrick Minnis, NASA Langley Research Center, MS 420, Hampton, VA 23681-2199. email: p.minnis@larc.nasa.gov.

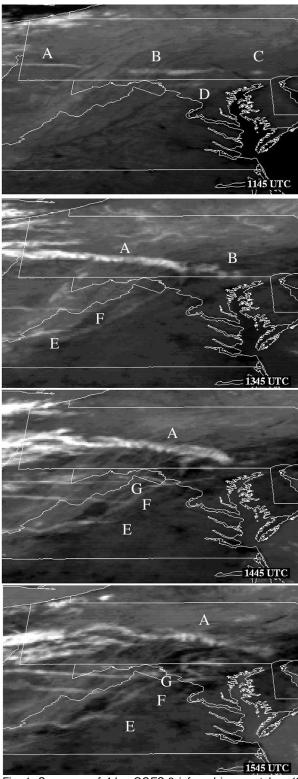


Fig. 1. Sequence of 4-km GOES-8 infrared images taken 12 Sept. 2001 showing developing contrails, 1145-1545 UTC.

time sequence. The roots of contrail A, which can be traced back at least to 0730 UTC over Illinois, are imbedded in the cirrus cloud seen over OH in Fig. 2.

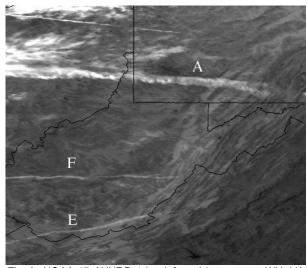


Fig. 2. NOAA-15 AVHRR 1-km infrared image over WV, VA, and PA, 1245 UTC 12 September 2001.

Additional contrails seen in the GOES-8 and NOAA-16 AVHRR imagery taken at or before 0730 UTC west of WV were observed to spread out, advect eastward, and dissipate by 1245 UTC. A few other significant contrails formed over PA and VA after 1545 UTC.

The contrail altitudes were estimated with stereography using GOES-8 with NOAA-14 and 15. At 1109 UTC, contrails A, B, and C were between 12 and 13.5 km. At 1245 UTC, contrails A, E, and F were located between 11 and 13 km, while contrails B and C were between 6.5 and 9.3 km. The eastern end of A, where it was breaking up, was between 8.5 and 9.3 km. The mean height of the north edge of A was 12.1 km, 1.5 km above the southern edge. The northern edges indicating

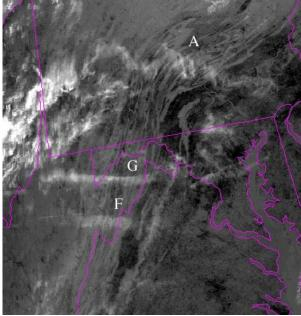


Fig. 3. Terra MODIS 1-km infrared image over WV, PA, MD, and VA, 1545 UTC 12 September 2001.

Table 1. Properties of contrails in Fig. 1, * denotes AVH	RR.
---	-----

Contrail, time (UTC) length (km) width (km) area (km²) optical depth A, 1015 329 5 1645 0.15 A, 1109* 325 6 1950 0.63 A, 1233* 309 21 6489 0.58 A, 1345 316 34 10744 0.30 A, 1545 323 25 8075 0.28 A, 2045 35 14 490 0.12 B, 1015 77 6 462 0.16 B, 1109* 190 9 1710 0.31 B, 1233* 197 23 4531 0.31 B, 1445 31 15 465 0.08 C, 1109* 16 40 640 0.26 C, 1233* 23 10 230 0.36 D, 1233* 85 10 850 0.25 E, 1345 346 15 5190 0.09 E, 1545 204 14 <th colspan="7">Table 1. Properties of contrails in Fig. 1, "denotes AVHRR.</th>	Table 1. Properties of contrails in Fig. 1, "denotes AVHRR.						
A, 1015 329 5 1645 0.15 A, 1109* 325 6 1950 0.63 A, 1233* 309 21 6489 0.58 A, 1345 316 34 10744 0.30 A, 1545 323 25 8075 0.28 A, 2045 35 14 490 0.12 B, 1015 77 6 462 0.16 B, 1109* 190 9 1710 0.31 B, 1233* 197 23 4531 0.31 B, 1445 31 15 465 0.08 C, 1109* 16 40 640 0.26 C, 1233* 23 10 230 0.36 D, 1233* 85 10 850 0.25 E, 1243* 401 5 2005 0.17 E, 1345 346 15 5190 0.09 E, 1545 204 14 2856 0.13 F, 1233* 316 5 1580 0.26			width				
A, 1109* 325 6 1950 0.63 A, 1233* 309 21 6489 0.58 A, 1345 316 34 10744 0.30 A, 1545 323 25 8075 0.28 A, 2045 35 14 490 0.12 B, 1015 77 6 462 0.16 B, 1109* 190 9 1710 0.31 B, 1233* 197 23 4531 0.31 B, 1445 31 15 465 0.08 C, 1109* 16 40 640 0.26 C, 1233* 23 10 230 0.36 D, 1233* 85 10 850 0.25 E, 1233* 401 5 2005 0.17 E, 1345 346 15 5190 0.09 E, 1545 204 14 2856 0.13 F, 1233* 316 5 1580 0.26 F, 1345 246 7 1722 0.12	time (UTC)	(km)	(km)	(km²)	depth		
A, 1233* 309 21 6489 0.58 A, 1345 316 34 10744 0.30 A, 1545 323 25 8075 0.28 A, 2045 35 14 490 0.12 B, 1015 77 6 462 0.16 B, 1109* 190 9 1710 0.31 B, 1233* 197 23 4531 0.31 B, 1445 31 15 465 0.08 C, 1109* 16 40 640 0.26 C, 1233* 23 10 230 0.36 D, 1233* 85 10 850 0.25 E, 1233* 401 5 2005 0.17 E, 1345 346 15 5190 0.09 E, 1545 204 14 2856 0.13 F, 1233* 316 5 1580 0.26 F, 1345 246 7 1722 0.12 F, 1545 237 14 3318 0.13	A, 1015	329	5	1645	0.15		
A, 1345 316 34 10744 0.30 A, 1545 323 25 8075 0.28 A, 2045 35 14 490 0.12 B, 1015 77 6 462 0.16 B, 1109* 190 9 1710 0.31 B, 1233* 197 23 4531 0.31 B, 1445 31 15 465 0.08 C, 1109* 16 40 640 0.26 C, 1233* 23 10 230 0.36 D, 1233* 85 10 850 0.25 E, 1233* 401 5 2005 0.17 E, 1345 346 15 5190 0.09 E, 1545 204 14 2856 0.13 F, 1233* 316 5 1580 0.26 F, 1345 246 7 1722 0.12 F, 1545 237 14 3318 0.13 F, 2015 90 11 990 0.12 G,	A, 1109*	325	6	1950	0.63		
A, 1545 323 25 8075 0.28 A, 2045 35 14 490 0.12 B, 1015 77 6 462 0.16 B, 1109* 190 9 1710 0.31 B, 1233* 197 23 4531 0.31 B, 1445 31 15 465 0.08 C, 1109* 16 40 640 0.26 C, 1233* 23 10 230 0.36 D, 1233* 85 10 850 0.25 E, 1233* 401 5 2005 0.17 E, 1345 346 15 5190 0.09 E, 1545 204 14 2856 0.13 F, 1233* 316 5 1580 0.26 F, 1345 246 7 1722 0.12 F, 1545 237 14 3318 0.13 F, 2015 90 11 990 0.12 G, 1445 267 7 1869 0.12 G, 15	A, 1233*	309	21	6489	0.58		
A, 2045 35 14 490 0.12 B, 1015 77 6 462 0.16 B, 1109* 190 9 1710 0.31 B, 1233* 197 23 4531 0.31 B, 1445 31 15 465 0.08 C, 1109* 16 40 640 0.26 C, 1233* 23 10 230 0.36 D, 1233* 85 10 850 0.25 E, 1233* 401 5 2005 0.17 E, 1345 346 15 5190 0.09 E, 1545 204 14 2856 0.13 F, 1233* 316 5 1580 0.26 F, 1345 246 7 1722 0.12 F, 1545 237 14 3318 0.13 F, 2015 90 11 990 0.12 G, 1445 267 7 1869 0.12 G, 1545 278 14 3892 0.24	A, 1345	316	34	10744	0.30		
B, 1015 77 6 462 0.16 B, 1109* 190 9 1710 0.31 B, 1233* 197 23 4531 0.31 B, 1445 31 15 465 0.08 C, 1109* 16 40 640 0.26 C, 1233* 23 10 230 0.36 D, 1233* 85 10 850 0.25 E, 1233* 401 5 2005 0.17 E, 1345 346 15 5190 0.09 E, 1545 204 14 2856 0.13 F, 1233* 316 5 1580 0.26 F, 1345 246 7 1722 0.12 F, 1545 237 14 3318 0.13 F, 2015 90 11 990 0.12 G, 1445 267 7 1869 0.12 G, 1545 278 14 3892 0.24	A, 1545	323	25	8075	0.28		
B, 1109* 190 9 1710 0.31 B. 1233* 197 23 4531 0.31 B, 1445 31 15 465 0.08 C, 1109* 16 40 640 0.26 C, 1233* 23 10 230 0.36 D, 1233* 85 10 850 0.25 E, 1233* 401 5 2005 0.17 E, 1345 346 15 5190 0.09 E, 1545 204 14 2856 0.13 F, 1233* 316 5 1580 0.26 F, 1345 246 7 1722 0.12 F, 1545 237 14 3318 0.13 F, 2015 90 11 990 0.12 G, 1445 267 7 1869 0.12 G, 1545 278 14 3892 0.24	A, 2045	35	14	490	0.12		
B. 1233* 197 23 4531 0.31 B, 1445 31 15 465 0.08 C, 1109* 16 40 640 0.26 C, 1233* 23 10 230 0.36 D, 1233* 85 10 850 0.25 E, 1233* 401 5 2005 0.17 E, 1345 346 15 5190 0.09 E, 1545 204 14 2856 0.13 F, 1233* 316 5 1580 0.26 F, 1345 246 7 1722 0.12 F, 1545 237 14 3318 0.13 F, 2015 90 11 990 0.12 G, 1445 267 7 1869 0.12 G, 1545 278 14 3892 0.24	B, 1015	77	6	462	0.16		
B, 1445 31 15 465 0.08 C, 1109* 16 40 640 0.26 C, 1233* 23 10 230 0.36 D, 1233* 85 10 850 0.25 E, 1233* 401 5 2005 0.17 E, 1345 346 15 5190 0.09 E, 1545 204 14 2856 0.13 F, 1233* 316 5 1580 0.26 F, 1345 246 7 1722 0.12 F, 1545 237 14 3318 0.13 F, 2015 90 11 990 0.12 G, 1445 267 7 1869 0.12 G, 1545 278 14 3892 0.24	B, 1109*	190	9	1710	0.31		
C, 1109* 16 40 640 0.26 C, 1233* 23 10 230 0.36 D, 1233* 85 10 850 0.25 E, 1233* 401 5 2005 0.17 E, 1345 346 15 5190 0.09 E, 1545 204 14 2856 0.13 F, 1233* 316 5 1580 0.26 F, 1345 246 7 1722 0.12 F, 1545 237 14 3318 0.13 F, 2015 90 11 990 0.12 G, 1445 267 7 1869 0.12 G, 1545 278 14 3892 0.24	B. 1233*	197	23	4531	0.31		
C, 1233* 23 10 230 0.36 D, 1233* 85 10 850 0.25 E, 1233* 401 5 2005 0.17 E, 1345 346 15 5190 0.09 E, 1545 204 14 2856 0.13 F, 1233* 316 5 1580 0.26 F, 1345 246 7 1722 0.12 F, 1545 237 14 3318 0.13 F, 2015 90 11 990 0.12 G, 1445 267 7 1869 0.12 G, 1545 278 14 3892 0.24	B, 1445	31	15	465	0.08		
D, 1233* 85 10 850 0.25 E, 1233* 401 5 2005 0.17 E, 1345 346 15 5190 0.09 E, 1545 204 14 2856 0.13 F, 1233* 316 5 1580 0.26 F, 1345 246 7 1722 0.12 F, 1545 237 14 3318 0.13 F, 2015 90 11 990 0.12 G, 1445 267 7 1869 0.12 G, 1545 278 14 3892 0.24	C, 1109*	16	40	640	0.26		
E, 1233* 401 5 2005 0.17 E, 1345 346 15 5190 0.09 E, 1545 204 14 2856 0.13 F, 1233* 316 5 1580 0.26 F, 1345 246 7 1722 0.12 F, 1545 237 14 3318 0.13 F, 2015 90 11 990 0.12 G, 1445 267 7 1869 0.12 G, 1545 278 14 3892 0.24	C, 1233*	23	10	230	0.36		
E, 1345 346 15 5190 0.09 E, 1545 204 14 2856 0.13 F, 1233* 316 5 1580 0.26 F, 1345 246 7 1722 0.12 F, 1545 237 14 3318 0.13 F, 2015 90 11 990 0.12 G, 1445 267 7 1869 0.12 G, 1545 278 14 3892 0.24	D, 1233*	85	10	850	0.25		
E, 1545 204 14 2856 0.13 F, 1233* 316 5 1580 0.26 F, 1345 246 7 1722 0.12 F, 1545 237 14 3318 0.13 F, 2015 90 11 990 0.12 G, 1445 267 7 1869 0.12 G, 1545 278 14 3892 0.24	E, 1233*	401	5	2005	0.17		
F, 1233* 316 5 1580 0.26 F, 1345 246 7 1722 0.12 F, 1545 237 14 3318 0.13 F, 2015 90 11 990 0.12 G, 1445 267 7 1869 0.12 G, 1545 278 14 3892 0.24	E, 1345	346	15	5190	0.09		
F, 1345 246 7 1722 0.12 F, 1545 237 14 3318 0.13 F, 2015 90 11 990 0.12 G, 1445 267 7 1869 0.12 G, 1545 278 14 3892 0.24	E, 1545	204	14	2856	0.13		
F, 1545 237 14 3318 0.13 F, 2015 90 11 990 0.12 G, 1445 267 7 1869 0.12 G, 1545 278 14 3892 0.24	F, 1233*	316	5	1580	0.26		
F, 2015 90 11 990 0.12 G, 1445 267 7 1869 0.12 G, 1545 278 14 3892 0.24	F, 1345	246	7	1722	0.12		
G, 1445 267 7 1869 0.12 G, 1545 278 14 3892 0.24	F, 1545	237	14	3318	0.13		
G, 1545 278 14 3892 0.24	F, 2015	90	11	990	0.12		
	G, 1445	267	7	1869	0.12		
G, 2015 79 23 1817 0.11	G, 1545	278	14	3892	0.24		
	G, 2015	79	23	1817	0.11		

a north-south wind shear below the contrail altitude. The unmarked trail north of A in Fig. 2 was estimated to be at 13 km. It dissipated within an hour. Trails A, B, and C advected at 74 kmh⁻¹ to the east-southeast between 1109 and 1239 UTC. Contrail B moved further south and had a more cellular structure than A. Contrail C was more amorphous than either A or B.

The dimensions of these trails, determined from the various satellite images, are summarized in Table 1. Most of the trails spread at 7-8 km h-1 and reached maximum width within 2-4 hours, except for G, which spread at about 5 kmh⁻¹ and peaked after only 2 hours from when it was first detectable. Contrails A, F, and G lasted more than 10 hours, while B dissipated after 5 hours. The contrail areal coverage reached a maximum of 20,456 km2 at 1445 UTC just from six contrails. The optical depths were computed using an assumed value of 220 K, which corresponds to an altitude of 11.5 km. Values of mean τ for each separate contrail vary from 0.08 to 0.63. The mean values weighted by the area of each contrail were 0.45 at 1109 and 1233 UTC and 0.22 at 1345 and 1545 UTC. The marked differences between the AVHRR-derived optical depths and those from GOES-8 may be due to the inability of detecting the cloud edge accurately from GOES, so that the mean contrail temperature may be overestimated and the areal coverage underestimated from GOES.

The values of RHI at 225 hPa (~12 km) plotted in Fig. 4 show one supersaturated area over central OH and Indiana at 1200 UTC and no areas at 1600 UTC.

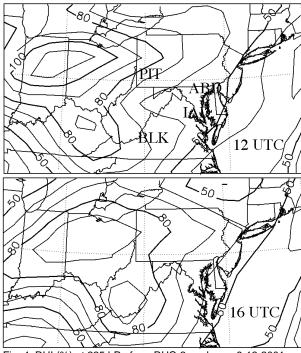


Fig. 4. RHI (%) at 225 hPa from RUC-2 analyses, 9-12-2001.

Over PA, RHI ranges from 90% at the OH border to 50% at the eastern PA border. Over Pittsburgh (PIT) underneath contrail A at 1200 UTC, the RUC RHI is 80%, while near Aberdeen, MD (ABD), close to C at 1200 UTC, RHI = 55%. A similar value is found over Dulles, VA (IAD) near contrail D, while RHI = 80% over Blacksburg, VA (BLK) near the end of E. These values are too low for sustaining contrails. To determine if these values are due to the model assimilation process, the rawinsonde RHI profiles are compared with the corresponding RUC values at 1200 UTC. in Fig. 5. The RUC increased RHI at most levels over BLK and PIT while smoothing or decreasing RHI over ABD and IAD. No contrails were observed for RHI < 55%.

None of the soundings show RHI > 72%, despite the fact that the PIT rawinsonde must have passed through contrail A on its way to the stratosphere. To support a persistent contrail, the maximum PIT RHI from the sonde would need to be increased by 35% or more. Another sounding taken over western OH yielded RHI = 117% at 225 hPa. Natural cirrus clouds were passing over the Wilmington, OH station at the time. Because it is theorized that natural cirrus clouds can only form adiabatically for RHI exceeding 145% or more (Sassen and Dodd 1989), the dry bias appears to be consistent in both clear and cloudy skies. To account for the dry bias, a correction formula was developed by assuming that most of contrails observed by Sassen (1997; his Fig. 5b) should have occurred only in supersaturated conditions. To include most of his contrail observations above a new line representing RHI = 100%, it is necessary to specify that RHI = 100% for the sonde value of RH = 16% at -70°C and RHI = 100% at RH = 72% and -36°C. The resulting formula is

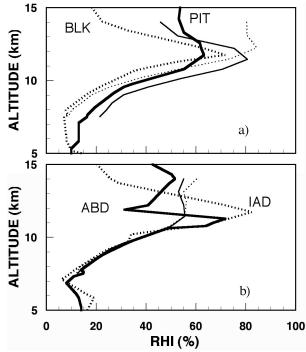


Fig. 5. RHI profiles at 12 UTC, 9-12-2001 from radiosondes (thick lines) and RUC-2 analyses (thin lines).

$$RHI_{cor} = RHI - 1.87 T + 443,$$
 (1)

where RHI is derived from rawinsonde measurements. Using this formula, valid only for T < 236K, the RHI profiles in Fig. 5 were recomputed and plotted in Fig. 6. Supersaturation occurs between 11 and 13 km for all four sites near the contrails observed in Figs. 1 and 2 around 1200 UTC. The profile over Wilmington, OH produced a maximum of $RHI_{cor} = 153$ %, a value that could support natural cirrus generation. Application of this correction formula to the RUC profiles would greatly expand the area of potential contrail coverage in Fig. 4. However, given the comparisons in Fig. 5, it is not clear that (1) can be applied directly to the RUC profiles.

To accurately simulate the contrails that would have formed during 12 September 2001, it is necessary to parameterize the spreading, lifetimes, and optical properties of the contrails based on the observations described here. The differences between the various contrails in Fig. 1 are probably directly related to the specific formation conditions as well as the subsequent conditions at each time step. For example, contrails B and C developed very rapidly, but appear to have precipitated quickly into drier layers. Figure 6 shows a relatively thin, very moist layer at 11.8 km. It is possible that the large values of RHI_{cor} would result in faster particle growth than for contrail A over PIT, where the supersaturated layer is thicker than over IAD, ABD, or BLK, but drier ($RHI_{cor} = 105\%$). Faster particle growth for B, C, and E would tend to cause precipitation into the dry layers below resulting in evaporation of the contrail at a much faster rate than seen for contrails A, F, and G.

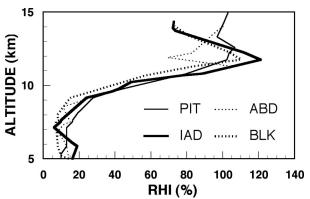


Fig. 6. As Fig. 5, except profiles of dry-bias corrected RHI, RHI_{con} from radiosonde profiles.

4. CONCLUDING REMARKS

The stoppage of air traffic over the USA permitted a detailed analysis of several persistent contrails developing in different conditions. After relating the contrail properties and life cycles to the atmospheric environment, a crude model will be developed to simulate the contrails and resulting cirrus cloudiness that would have occurred if air traffic had been normal.

REFERENCES

Benjamin, S. G., J. M. Brown, K. J. Brundage, B. E. Schwartz, T. G. Smirnova, and T. L. Smith, 1998: The operational RUC-2. *Proc. AMS 16th Conf Weather Analysis and Forecasting*, Phoenix, AZ, 249-252.

Duda, D. P., P. Minnis, P. K. Costulis, and R. Palikonda. 2002: An estimation of US contrail frequency from RUC and flight track data. *Proc. AMS* 10th Conf. Aviation, Range, and Aerospace Meteor., Portland, OR, May 13-16.

Minnis, P., J, K, Ayers, R. Palikonda, D. R. Doelling, U. Schumann, and K. Gierens, 2001: Changes in cirrus cloudiness and their relationship to contrails. *Proc. AMS 12th Symp. Global Change Studies and Climate Variations*, Albuquerque, NM, Jan. 15-19, 239-242.

Minnis, P., J. K. Ayers, and S. P. Weaver, 2002: Contrail frequency over the USA from surface observations. Submitted to *Geophys. Res. Lett.*

Minnis, P., D. F. Young, L. Nguyen, D. P Garber, W. L. Smith, Jr., and R. Palikonda, 1998: Transformation of contrails into cirrus during SUCCESS. *Geophys. Res. Ltrs.*, 25, 1157-1160.

Palikonda, R. and P. Minnis, 2002: Contrail climatology over the USA from MODIS and AVHRR data. Proc. AMS 10th Conf. Aviation, Range, and Aerospace Meteor., Portland, OR, May 13-16.

Sassen, K., 1997: Contrail cirrus and their potential for regional climate change. *Bull. Amer. Meteor. Soc.*, 78, 1885-1903.

Sassen, K. and G. C. Dodd, 1989: Haze particle nucleation simulations of cirrus clouds, and applications for numerical and lidar studies. *J. Atmos. Sci.*, **46**, 3005-3014.